International Journal of Biological Macromolecules 51 (2012) 25–31

Contents lists available at SciVerse ScienceDirect

International Journal of Biological Macromolecules

journal homepage: www.elsevier.com/locate/ijbiomac

Fumarate hydratase isoforms of *Leishmania major*: Subcellular localization, structural and kinetic properties

Patrícia R. Feliciano[a], Shreedhara Gupta[b], Fabio Dyszy[c], Marcelo Dias-Baruffi[d], Antonio J. Costa-Filho[e], Paul A.M. Michels[b], M. Cristina Nonato[a,*]

[a] *Laboratório de Cristalografia de Proteínas, FCFRP, Universidade de São Paulo, Ribeirão Preto 14040-903, Brazil*
[b] *Research Unit for Tropical Diseases, de Duve Institute and Laboratory of Biochemistry, Université catholique de Louvain, B-1200 Brussels, Belgium*
[c] *Grupo de Biofísica Molecular Sergio Mascarenhas, IFSC, Universidade de São Paulo, São Carlos 13560-970, Brazil*
[d] *Laboratório de Glicoimunobiologia, FCFRP, Universidade de São Paulo, Ribeirão Preto 14040-903, Brazil*
[e] *Laboratório de Biofísica Molecular, Departamento de Física, FFCLRP, Universidade de São Paulo, Ribeirão Preto 14040-901, Brazil*

ARTICLE INFO

Article history:
Received 21 February 2012
Received in revised form 19 April 2012
Accepted 27 April 2012
Available online 5 May 2012

Keywords:
Fumarate hydratase
Leishmania major
cell compartmentalization
kinetics
structure

ABSTRACT

Fumarate hydratases (FHs; EC 4.2.1.2) are enzymes that catalyze the reversible hydration of fumarate to S-malate. Parasitic protists that belong to the genus *Leishmania* and are responsible for a complex of vector-borne diseases named leishmaniases possess two genes that encode distinct putative FH enzymes. Genome sequence analysis of *Leishmania major* Friedlin reveals the existence of genes LmjF24.0320 and LmjF29.1960 encoding the putative enzymes *Lm*FH-1 and *Lm*FH-2, respectively. In the present work, the FH activity of both *L. major* enzymes has been confirmed. Circular dichroism studies suggest important differences in terms of secondary structure content when comparing *Lm*FH isoforms and even larger differences when comparing them to the homologous human enzyme. CD melting experiments revealed that both *Lm*FH isoforms are thermolabile enzymes. The catalytic efficiency under aerobic and anaerobic environments suggests that they are both highly sensitive to oxidation and damaged by oxygen. Intracellular localization studies located *Lm*FH-1 in the mitochondrion, whereas *Lm*FH-2 was found predominantly in the cytosol with possibly also some in glycosomes. The high degree of sequence conservation in different *Leishmania* species, together with the relevance of FH activity for the energy metabolism in these parasites suggest that FHs might be exploited as targets for broad-spectrum antileishmanial drugs.

1. Introduction

Human leishmaniases are parasitic diseases caused by about 20 species of the genus *Leishmania*, obligate intramacrophage protists transmitted by about 30 species of phlebotomine sandflies [1]. The main clinical manifestations of leishmaniases are ulcerative skin lesions, destructive mucosal inflammation, and disseminated visceral infection [2]. Leishmaniases, classified as neglected tropical diseases, are a global health problem and threaten 350 million people in 88 countries around the world. The World Health Organization has estimated that 12 million people are currently infected, with 2 million new cases each year. There is no vaccine available for preventing leishmaniasis [3] and the current treatment is mainly based on pentavalent antimonials and second line drugs such as amphotericin B and pentamidine. However, the current antileishmanial therapy displays serious side effects due to toxicity, the costs of adequate therapy are high and cases of drug resistance have already been reported. There is an urgent need for development of novel, efficacious, safe and affordable anti-parasitic agents to prevent, control and treat leishmaniases.

Genome sequencing projects of *Leishmania major* [4], *Leishmania infantum* [5] and *Leishmania braziliensis* [5] have been completed and have allowed to understand similarities and differences among different *Leishmania* species, thus making an important contribution to the identification of new drug targets and vaccine candidates for leishmaniases [6].

In the particular case of the study reported in this paper, the analysis of the available *L. major* genome sequence has led to the identification of two genes, LmjF24.0320 and LmjF29.1960, which encode distinct putative fumarate hydratases (FHs; EC 4.2.1.2), enzymes also called fumarases, which catalyze the stereospecific reversible hydration of fumarate to S-malate.

Abbreviations: FH, fumarate hydratase; *Lm*FH, fumarate hydratase from *Leishmania major*; *Lm*FH-1, fumarate hydratase from *L. major* encoded by LmjF24.0320 gene; *Lm*FH-2, fumarate hydratase from *L. major* encoded by LmjF29.1960 gene.

* Corresponding author. Tel.: +55 16 3602 4432; fax: +55 16 3602 4880.
E-mail address: cristy@fcfrp.usp.br (M.C. Nonato).

0141-8130
http://dx.doi.org/10.1016/j.ijbiomac.2012.04.025

Fumarate hydratases (FHs) have been initially grouped into two classes depending on their thermal stability, relative subunit arrangement, and metal requirement [7]. Class I fumarate hydratases are oxygen-sensitive, thermolabile, homodimeric, Fe–S cluster containing enzymes with a molecular mass of approximately 120 kDa, and can occur in bacteria (fumA and fumB from *Escherichia coli* [7]) and at least several groups of unicellular eukaryotes [8]. Class II fumarate hydratases are oxygen-insensitive, thermostable, iron-independent, homotetrameric enzymes of 200 kDa, and occur in bacteria (fumC from *E. coli* [7]) and higher eukaryotes such as mammals [9,10]. Although functionally related, FHs from classes I and II exhibit low sequence identity (around 20%). Recently, a novel group of fumarate hydratases has been described in the literature as two-subunit FHs based on sequence identity to class I fumarate hydratases [11,12]. Two-subunit fumarate hydratases are oxygen-sensitive, thermostable, Fe–S cluster-containing heterodimeric proteins with two different subunits (α and β subunit).

In general, eukaryotic cells express two isoforms of fumarate hydratase: a cytosolic and a mitochondrial one. The cytosolic isoform has been suggested to be involved in the production of fumarate that acts as a substrate for dihydroorotate dehydrogenase, an enzyme involved in the *de novo* pyrimidine biosynthesis pathway [13,14]. Furthermore, the cytosolic fumarate hydratase has also been described as being able to migrate from the cytosol to the nucleus where it plays a key role in DNA repair. In humans, the deficiency of this fumarate hydratase is related to a tumor susceptibility syndrome, Hereditary Leiomyomatosis and Renal Cell Cancer (HLRCC) [15].

The mitochondrial isoform participates in the tricarboxylic acid (TCA) cycle and may also take part in the succinic fermentation pathways providing fumarate for the enzyme fumarate reductase [16]. In humans, mutations in the mitochondrial fumarate hydratase are responsible for the Fumarase Deficiency disease, also known as fumaric aciduria, described as a severe encephalopathy that leads to seizures and developmental delay [17].

While there are a wide range of studies focusing on the human enzymes, from biophysicochemical and structural characterization to their involvement in cellular functions, there is very limited information available on the possible role of fumarate hydratases in other organisms. To our knowledge, the data available to Trypanosomatidae, the protist family comprising parasites such as *Leishmania* and *Trypanosoma*, are limited to a RNA interference study that showed that fumarate hydratase activity is essential for the viability of the insect-stage specific procyclic form of the human sleeping-sickness causing parasite *Trypanosoma brucei* [18].

It is our interest to investigate the role of fumarate hydratases in *Leishmania*. As a first step towards this goal, we report here the cloning, heterologous expression, purification and characterization of the products of two genes from *L. major* (LmjF24.0320 and LmjF29.1960), each encoding a putative fumarate hydratase enzyme, *Lm*FH-1 and *Lm*FH-2, respectively, of which we confirmed the predicted activity. Subcellular localization studies showed that the *Lm*FH isoforms are localized in different cell compartments, *Lm*FH-1 being mitochondrial and *Lm*FH-2 showing its localization essentially in the cytosol and possibly also some in glycosomes, the characteristic peroxisome-like organelles of Kinetoplastea, the protist clade to which trypanosomatids belong. The biophysical and biochemical characterization showed that *Lm*FH-1 and *Lm*FH-2 follow Michaelis–Menten kinetics and display differences in protein folding. The study here presented provides the first data on fumarate hydratases from *Leishmania*, significantly contributing to the understanding of the functional role of these enzymes in that parasite.

2. Materials and methods

2.1. Cloning, expression and purification of recombinant LmFH isoforms

The open-reading frames encoding full-length *Lm*FH isoforms were amplified by PCR using as a template genomic DNA, isolated from promastigote forms of *L. major* Friedlin. Two pairs of oligonucleotides, forward primer 5′-GACGACGAATTCATGCTCCGCCGCCTTGC-3′ and reverse primer 5′-GACGACGCGGCCGCACTAGAGCTGTTCGAAGAAGTCGTTG-3′, and forward primer 5′-GACGACGAATTCATGTCTCTGTGCGACCAGTGC-3′ and reverse primer 5′-GACGACGCGGCCGCATCACGCAA GCGTCTTCGAGTACAT-3′, were, respectively, based on the sequences of the genes putatively annotated as *FH*s in the *L. major* genome database (accession codes LmjF24.0320 and LmjF29.1960) and designed to introduce *Eco*RI and *Not*I restriction sites (underlined). The PCR for each FH gene was carried out in a 50 μl volume containing 0.4 μM of each primer, 0.5 ng μl^{-1} of genomic DNA, 2 mM $MgSO_4$ (Invitrogen), 0.2 mM dNTP mixture (Invitrogen) and 1 U of Platinum Taq DNA polymerase High Fidelity (Invitrogen). The reactions were performed by initial denaturation at 94 °C for 120 s followed by 25 cycles of 94 °C for 30 s (denaturation), 60 °C for 30 s (annealing), and 68 °C for 120 s (elongation), final extension was performed at 68 °C for 10 min. The resulting PCR products were visualized on a 0.8% agarose gel stained with ethidium bromide, gel extracted, and purified using a QIAquick Gel Extraction Kit (Qiagen). The purified PCR products were digested with *Eco*RI (Invitrogen) and *Not*I (Invitrogen) to provide cohesive ends and ligated to digested expression vector pET-28a (Novagen) using T4 DNA ligase (Invitrogen). *E. coli* DH5α competent cells were transformed with the ligated mixtures, clones selected and the plasmids propagated [19]. Plasmid DNA was extracted from the transformants using the QIAprep spin Miniprep Kit (Qiagen) and the sequences of the cloned genes were confirmed by DNA sequencing. One sequenced clone of each FH gene was selected and used to transform *E. coli* strain BL21(DE3) cells. The full-length *Lm*FH isoforms were expressed as histidine-tagged fusion proteins. A single colony of *E. coli* BL21(DE3) cells harboring a recombinant *Lm*FH plasmid was used to inoculate 10 ml Luria-broth (LB) medium supplemented with 30 μg ml^{-1} kanamycin and the culture was grown for 16 h at 37 °C with shaking. The culture was then 1:100 diluted with LB containing 30 μg ml^{-1} kanamycin and grown at 37 °C till the OD_{600nm} reached 0.5–0.6. The cells were then induced with 0.25 mM isopropyl β-D-thiogalactopyranoside (IPTG), the culture supplemented with 2 mM cysteine, 0.2 mg ml^{-1} ferrous sulfate, 0.2 mg ml^{-1} ferric citrate [20], and growth was continued for 24 h at 18 °C. The induced culture was harvested by centrifugation at 6800 × *g* for 10 min. The bacterial pellet obtained from 1 l of culture was frozen at −20 °C. The cells were suspended into 20 ml buffer A (50 mM sodium phosphate, pH 8.5, 300 mM NaCl) with 1 mM phenylmethylsulfonyl (PMSF) and lysed by sonication with 10 × 30 s bursts (with 30 s intervals between each burst) using a Misonix XL 2000 sonicator fitted with a microtip probe and set at power setting 4. The crude extract was clarified by centrifugation at 15,700 × *g* for 15 min at 4 °C. The enzyme *Lm*FH, present in the soluble fraction, was loaded on a 2 ml column of Ni–NTA resin (Qiagen) equilibrated with buffer A. The column was then washed with a step gradient of imidazole from 0 to 50 mM in buffer A. The recombinant *Lm*FH was eluted with buffer A containing 100 mM imidazole; the purity of the protein was checked by 12% SDS–PAGE and its concentration determined by UV absorbance spectroscopy at 280 nm [21] (ε_{280nm} = 42,790 M^{-1} cm^{-1} for *Lm*FH-1 and ε_{280nm} = 65,500 M^{-1} cm^{-1} for *Lm*FH-2). All steps of the purification were performed in either aerobic or anaerobic conditions, in the latter case using a glove box supplied with nitrogen gas.

2.2. Circular dichroism (CD)

Far-UV CD spectra (195–250 nm) of the *Lm*FH isoforms were measured in a JASCO J-715 spectropolarimeter equipped with a temperature controller. The measurements were performed with temperature variation (10–94 °C), 0.2 mg ml^{-1} protein in 4–5 mM Tris, pH 8.5, 4–5 mM NaCl and using a 1 mm path length quartz cell, 100 nm min^{-1} scanning speed, 2 nm band width, 2 s response time, 0.2 nm data pitch. At the end of each thermal scan, the LmFH-1 and LmFH-2 samples were allowed to cool to 10 °C before rescanning to assess reversibility/irreversibility of the unfolding reaction. The final spectrum was the average of four scans. The CD spectrum was converted to mean molar ellipticity per residue $[\theta]_\lambda = (\theta_\lambda\, M_0)/(10\, lc)$, where θ_λ is the experimental ellipticity in millidegrees, M_0 is the mean molecular weight per residue (M_0 = 115), c is the protein concentration (mg ml^{-1}), and l is the path length (cm).

2.3. Optimum pH and enzymatic kinetics of LmFH isoforms

All studies were performed with the oligo-histidine tagged enzyme; the *Lm*FH activity measurements were carried out in either aerobic or anaerobic conditions, in the latter case using a glove box supplied with nitrogen gas. The fumarate production or consumption was measured spectrophotometrically at 250 nm (ε = 1450 M^{-1} cm^{-1}) at room temperature in a Hitachi U-2800 spectrophotometer. The pH dependence of activity was determined by varying the pH of the reaction mixtures (50 mM sodium acetate, pH 4 and 5, 50 mM sodium cacodylate, pH 6.2, 50 mM Tris, pH 7, 8, and 9, 50 mM glycine/NaOH, pH 10, 50 mM $NaHCO_3$/NaOH, pH 11, 50 mM KCl/NaOH, pH 12, with 150 mM NaCl) using 1 mM substrate, S-malate or fumarate, in a total volume of 1 ml. The kinetic parameters, V_{max} and K_m, were determined from a Lineweaver–Burk plot fitted to the experimental data obtained by varying the concentration of S-malate using 0.125, 0.25, 0.5, 1, 2, 4 and 8 mM, and varying the concentration of fumarate using 31.25, 62.5, 125, 250, 500 and 1000 μM. Kinetic assays were performed in a reaction mixture containing 50 mM Tris, pH 8.5 (*Lm*FH-1) and 9 (*Lm*FH-2), 150 mM NaCl with substrate, S-malate or fumarate, in a total volume of 1 ml. All studies were performed with the *Lm*FH (40 μg ml^{-1} final concentration) in 50 mM Tris, pH 8.5, 150 mM NaCl.

2.4. Production of purified polyclonal antibodies to LmFH isoforms

The production of polyclonal antisera against *Lm*FH-1 and *Lm*FH-2 was performed by immunization of rabbits with 800 μg of recombinant protein in PBS, pH 7.4. Rabbits were given initial intradermal injections at five spots in dorsal muscles with recombinant protein emulsified in complete Freund's adjuvant. At 15, 30 and 45 days after the initial injection, the rabbits were given booster intramuscular injections with the same antigen emulsified with Freund's incomplete adjuvant. Before each immunization, blood was collected, clotted at room temperature for 1 h, centrifuged at 450 × *g* for 15 min at 4 °C, and the sera were stored at −20 °C. 15 days after the last immunization, antibodies in the sera were precipitated with 40% ammonium sulfate, redissolved and dialyzed against PBS, pH 7.4, for 3 days. IgG antibodies against *Lm*FH-1 and *Lm*FH-2 were purified by affinity chromatography on a protein G column (IgG anti-*Lm*FH-1 and IgG anti-*Lm*FH-2). The column was equilibrated and washed with PBS, pH 7.4. The antibodies were eluted with 0.2 M glycine pH 2.8 and neutralized with 1 M K_2HPO_4 pH 10. The development of anti-*Lm*FH-2 and anti-*Lm*FH-2 polyclonal antibodies was monitored by enzyme-linked immunosorbent assay (ELISA).

2.5. Subcellular localization in Leishmania mexicana mexicana

2.5.1. Parasites

Leishmania mexicana mexicana promastigotes (MHOM/BZ/84/BEL46) were grown *in vitro* at 28 °C in a semi-defined medium (SDM-79) supplemented with 10% fetal calf serum.

2.5.2. Subcellular fractionation by treatment of cells with digitonin

Parasites were centrifuged at 400 × *g* for 10 min, washed twice in SHE buffer (25 mM HEPES, pH 7.4, 250 mM sucrose, 1 mM EDTA) containing a protease inhibitor cocktail (1 μM pepstatin, 1 μM leupeptin, 10 μM AEBSF, 100 μM EDTA) and resuspended in 1 ml of the same solution. 100 μl of cell suspension were incubated with 0.1% Triton X-100 (v/v) at 4 °C for 20 min and the total protein concentration was estimated by the Bradford assay [22]. Aliquots of cell suspensions containing 300 μg of protein were diluted in HBSS buffer (1.3 mM $CaCl_2$, 5 mM KCl, 0.3 mM KH_2PO_4, 0.5 mM $MgCl_2$, 0.4 mM $MgSO_4$, 138 mM NaCl, 4 mM $NaHCO_3$, 0.3 mM $NaHPO_4$, 15 mM HEPES, pH 7.1) and digitonin (0.01–1 mg digitonin/mg protein) in a 300 μl final volume. The cells were incubated at 25 °C for 4 min. As control of total release of enzymes from all compartments, parasites were incubated with 0.1% Triton X-100 (v/v) in HBSS buffer for 20 min at 4 °C. The cells were then centrifuged at 13,000 × *g* for 2 min at 4 °C, and supernatants and insoluble fractions (resuspended in 300 μl HBSS buffer) were utilized for western blot and activity analysis of proteins released from different cell compartments. The activity of enolase (E.C.4.2.1.11) and hexokinase (E.C.2.7.1.1) was measured as described previously [23,24].

2.5.3. Western blot

Supernatants and insoluble fractions obtained by subcellular fractionation with digitonin and Triton X-100 were analyzed by 10% SDS-PAGE and the proteins were subsequently transferred from the gel to a nitrocellulose membrane. The membranes were blocked with 5% milk in PBS for 12 h at 4 °C, washed with PBS and incubated with the appropriate primary antibodies (anti-*Lm*FH-1 at 1:4000, anti-*Lm*FH-2 at 1:8000 and anti-TIM at 1:50,000) for 1 h at room temperature. After washes with PBS, the membranes were incubated with as secondary antibody anti-rabbit IgG conjugated to horseradish peroxidase (1:10,000) for 1 h at room temperature, and visualized with the Western Blotting System (Pierce).

2.5.4. Immunofluorescence confocal microscopy

L. mexicana mexicana cells were stained with 0.3 nM Mito-Tracker Red CMXRos (Molecular Probes) for 30 min at 28 °C. Cells were fixed with 4% formaldehyde in PBS for 10 min, permeabilized with 1% Triton X-100 for 15 min and incubated with 0.1 M glycine in PBS for 12 h at 4 °C. The parasites were added onto poly-lysine coated slides, incubated for 1 h at room temperature and then incubated with 5% BSA in PBS for 45 min at 37 °C. Then primary antibodies (anti-*Lm*FH-1 at 1:1000 and anti-*Lm*FH-2 at 1:500) in PBS containing 2% BSA were added to cells and incubated for 45 min at 37 °C. After washing with PBS, secondary antibody (1:800 Alexa Fluor 488 anti-rabbit IgG and 1:1000 TO-PRO (DNA marker) – Molecular Probes) in PBS containing 2% BSA were added and incubated (45 min at 37 °C). The cells were washed, mounted in Mowiol and visualized using a Zeiss Axiovert microscope coupled to an MRC-1024 confocal scanning laser imaging system (Bio Rad).

3. Results and discussion

3.1. In silico analysis of LmFH sequences

Analysis of the *L. major* genome sequence has led to the identification of two genes, LmjF24.0320 and LmjF29.1960, which encode distinct putative fumarate hydratase enzymes, *Lm*FH-1 and *Lm*FH-2, respectively. Sequence analysis indicated that *Lm*FH-1 and *Lm*FH-2 share approximately 63% identity, are both members of class I fumarate hydratases, and exhibit, respectively, 15% and 17% amino-acid sequence identity to the homologous human enzyme.

These two class I fumarate hydratases are highly conserved among *Leishmania* species with the amino acid sequence identity varying from 91 to 99% (Supplementary Figs. S1 and S2). This high degree of sequence conservation suggests an important role for both isoforms within the genus *Leishmania* and raises the question what would be the specific role of each enzyme, including whether the differences and similarities are related to their localization in the cell, preference and affinity for substrates, and levels of protein expression in different life-cycle forms of *Leishmania.*

Sequence analysis with TargetP (http://www.cbs.dtu.dk/services/TargetP) of the *Lm*FH-1 isoform allowed the identification of a putative mitochondrial transit peptide. Moreover a candidate type 2 peroxisomal-targeting signal (PTS2) was detected near the N-terminus (KVSHKETKY), just downstream of the mitochondrial transit peptide. This PTS could potentially route the enzyme also to the glycosomes [25]. It has been suggested that the *Lm*FH-2 isoform might also be targeted to glycosomes since it contains a cryptic PST1 at its C-terminal extremity (SKTLA) [26]. Analyzing, in addition, the sequence similarity between each of the *Leishmania* isoforms and the orthologous enzymes from *T. brucei*, a high degree of identity can be found between *Lm*FH-1 and the mitochondrial isoform *Tb*FHm (76.4%) and *Lm*FH-2 and the cytosolic isoform *Tb*FHc (72.7%). Furthermore, the different predicted targeting signals are almost fully conserved amongst all *Leishmania* species analyzed (Supplementary Figs. S1 and S2) and are also present in all available corresponding FH sequences from *Trypanosoma* species.

These results together suggest the presence of *Lm*FH-1 in the mitochondrion and *Lm*FH-2 in the cytosol and do not rule out the possibility of a dual localization for both isoforms involving also the glycosomes.

3.2. Cloning, expression and purification of recombinant LmFH isoforms

The open-reading frames encoding the full-length isoforms *Lm*FH-1 and *Lm*FH-2 were amplified by the polymerase chain reaction (PCR) using genomic DNA as a template. The amplified products of 1650 and 1707 bp encode proteins with 549 (61.1 kDa) and 568 (62.6 kDa) amino acids, respectively. The amplified genes were ligated in plasmid pET-28a, into its *Eco*RI and *Not*I restriction sites. The *Lm*FH isoforms were overexpressed as soluble, active proteins in *E. coli* strain BL21(DE3). The purification of the recombinant *Lm*FH isoforms was performed by affinity chromatography with a Ni–NTA resin. The final products were shown to be homogeneous by SDS-PAGE (Supplementary Fig. S3). Approximately 5 mg of *Lm*FH-1 and 10 mg of *Lm*FH-2 could be obtained from 1 l cultures.

3.3. Circular dichroism (CD)

Far-UV circular dichroism spectra for the *Lm*FH isoforms as a function of the temperature are presented in Fig. 1, panels A and C. The circular dichroism spectra were characterized by two negative bands at 208 and 220 nm and a positive band at 195 nm. The minimum at 220 nm was mainly attributed to helical structures, while the negative band around 210 nm was probably the result of a mixture of the minimum at 208 nm arising from a helix structure with the band at 215 nm originating from β-sheets, which suggested a protein structure of type α/β. Moreover, the comparable intensity of the band at 208 nm and the maximum at 197 nm and minimum around 220 nm indicate substantial quantities of β-sheets.

The prediction of secondary structure content was performed by deconvolution of the CD spectra of *Lm*FH-1 and *Lm*FH-2 using K2D2 [27]. The secondary structure content was estimated as 29% α-helix and 18% β-sheet for *Lm*FH-1 and 28% α-helix and 26% β-sheet for *Lm*FH-2 (both at 20 °C), suggesting that these proteins, although both belonging to class 1, may show difference in folding. Even so, the absolute value of secondary structure content can slightly change depending on which algorithm has been used, differences between LmFH-1 and LmFH-2 structure content can be clearly observed. Our results are very different from those reported for class II fumarate hydratase, which showed a secondary structure content of 56.5% α-helix and 13.1% β-sheet [28], indicating that fumarate hydratases from class I and II probably have important structural differences.

Thermal denaturation of LmFH-1 and LmFH-2 showed that the proteins gradually lose their secondary structure, reaching complete loss of this content at 70 °C. The behavior of molar ellipticity as a function of temperature at 222 (Fig. 1B) and 220 nm (Fig. 1D) indicate melting temperatures of 56.3 °C for LmFH-1 and 57.7 °C for LmFH-2, respectively. The thermal stability observed implies that the LmFH isoforms can be considered thermolabile enzymes, especially when compared to the class 2 thermostable enzymes where the T_m values can reach 80–90 °C [29–31].

Comparing with the initial values, analysis of the spectral rescan after the complete run of thermal scan confirmed a significant loss of α-helix content and β-strand structure, and an increase in unordered content. In addition, macroscopically observable precipitates can be observed upon removal of LmFH samples from the instrument. Together those results suggest the irreversibility nature of thermal denaturation for both LmFHs.

3.4. Kinetic characterization of the LmFH isoforms

The optimum pH values for activity were estimated to be approximately 8.7 and 9 for *Lm*FH-1 and *Lm*FH-2, respectively, for the reactions in both directions. These results correlate quite well with values reported for class I enzymes from other organisms: *c.f.* fumarate hydratase from *Euglena gracilis var. bacillaris* (pH 8.4) [8] and fumarate hydratase from bacterium strain MPOB (pH 8.5) [32].

Values of the kinetic parameters, K_m, V_{max} and k_{cat} were determined from Lineweaver–Burk plots at pH 8.5 and 9 for *Lm*FH-1 and *Lm*FH-2, respectively, under anaerobic and aerobic conditions. The K_m and V_{max} values of the *Lm*FH isoforms for S-malate and fumarate are shown in Table 1. The results demonstrate that the K_m values of *Lm*FH-2 are approximately 2-fold higher than those of *Lm*FH-1 for fumarate, and 5-fold for S-malate. Our results show that the *Lm*FHs have higher K_m values than those reported for other class I enzymes: fumarate hydratase A from *E. coli* (K_m = 0.6 mM for fumarate and K_m = 0.7 mM for malate) [33], fumarate hydratase from *E. gracilis var. bacillaris* (K_m = 0.031 mM for fumarate and K_m = 0.14 mM for malate) [8] and fumarate hydratase from bacterium strain MPOB (K_m = 0.25 mM for fumarate and K_m = 2.38 mM for malate) [32]. This comparison between K_m values suggests that both *Lm*FHs have affinities for both substrates, fumarate and malate, lower than the other class I FHs. The low affinity for malate has also been reported for malate dehydrogenase isozymes in *L. major* [34], suggesting that the concentrations of these metabolites in *Leishmania* spp. can be relatively high.

The catalytic efficiency estimated by determining the k_{cat} values in both aerobic and anaerobic conditions suggests that the

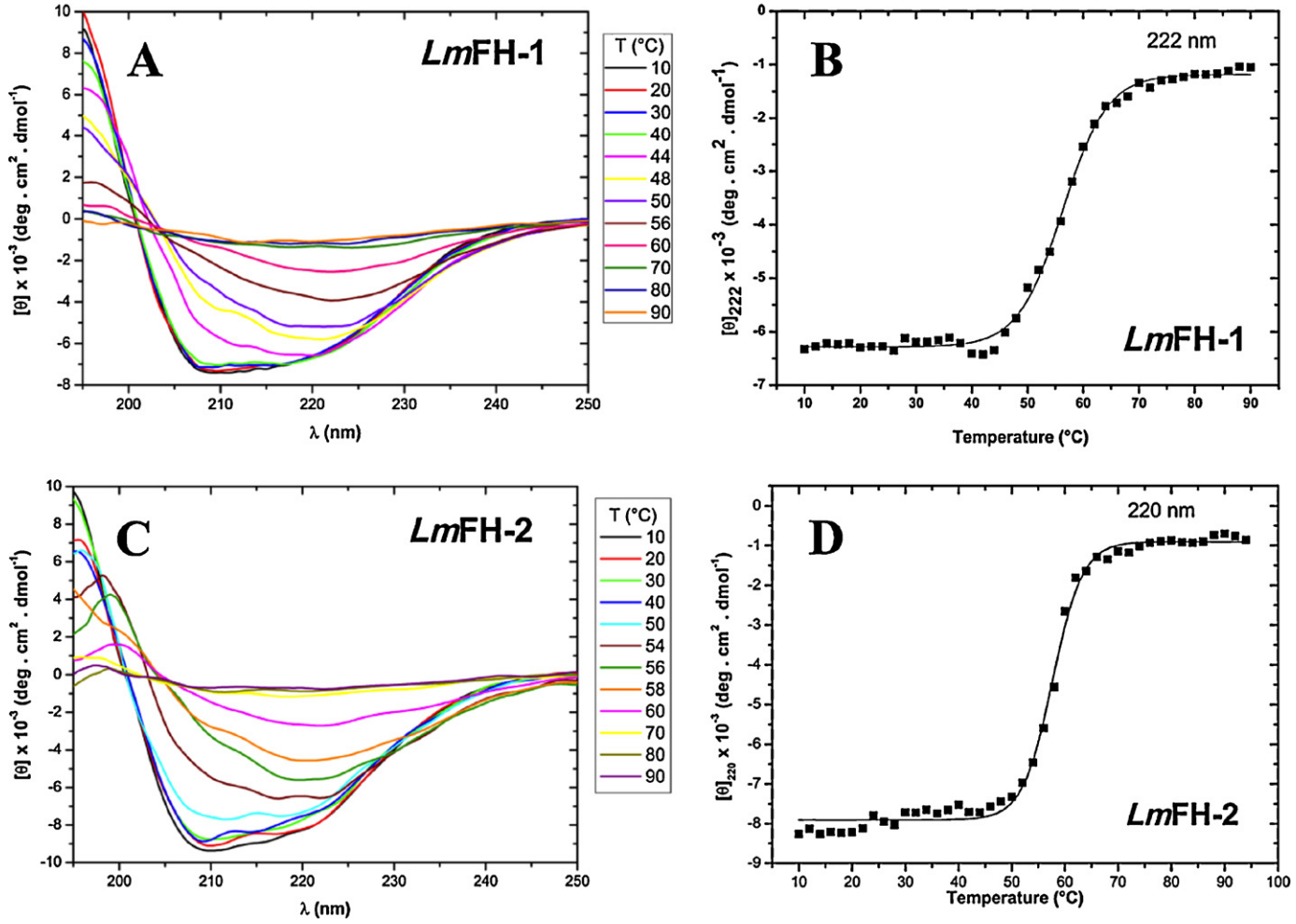

Fig. 1. Circular dichroism spectra of *Lm*FH-1 (A) and *Lm*FH-2 (C) at different temperatures. Thermal denaturation of *Lm*FH proteins monitored by molar ellipticity at 222 (B – *Lm*FH-1) and 220 nm (D – *Lm*FH-2) as a function of temperature. In panels B and D, the solid line is a fit to a two-state model that only serves as a guide for the eye.

enzymes are sensitive to oxygen leading to a 2- to 12-fold reduction in catalytic efficiency, depending on the isoform and the substrate considered. The inactivation by oxygen is a characteristic of class I fumarate hydratases that contain a catalytically active $[4Fe–4S]^{2+}$ cluster [32,35], which can be oxidized by oxygen leading to formation of an inactive $[3Fe–4S]^{+}$ cluster.

3.5. Intracellular localization of the LmFH isoforms

The intracellular localization of the FH isoforms was studied in cultured insect-stage, promastigote forms of *L. mexicana* by subcellular fractionation through selective membrane permeabilization with the detergent digitonin and by immunofluorescence microscopy. The different membranes were successively permeabilized by increasing concentrations of digitonin. Soluble and insoluble fractions of *L. mexicana* obtained with different concentrations of digitonin were analyzed by western blots using anti-*Lm*FH-1, anti-*Lm*FH-2 and anti-TIM (triosephosphate isomerase, a glycosomal matrix marker protein) sera (Fig. 2A).

Soluble fractions were also utilized to measure the activities of the enzymes hexokinase (glycosomal marker), enolase (cytosolic marker) and fumarate hydratase (Fig. 2B). Activity assays indicated that both fumarate hydratase and enolase were released from cells treated with digitonin concentrations as low as 0.1 mg per mg of protein. The hexokinase activity measurements combined with western blot analysis of TIM protein indicated that glycosomal proteins were released starting at concentrations of 0.5 mg of digitonin per mg of protein. Monitoring of fumarate hydratase activity indicated a small increase of released *L. mexicana* FH from 0.5 mg of digitonin per mg of protein, suggesting the presence of some

Table 1
Kinetic parameters of the *Lm*FH isoforms.

Enzyme	Substrate	K_m (mM)	V_{max} (μmol min^{-1} mg^{-1})	k_{cat} (s^{-1})	Reaction condition
*Lm*FH-1	Fumarate	2.5 ± 0.4	26.4 ± 4.4	28.3 ± 4.7	Anaerobic
*Lm*FH-1	Fumarate	1.3 ± 0.3	1.8 ± 0.3	1.9 ± 0.3	Aerobic
*Lm*FH-2	Fumarate	5.7 ± 1.4	186.2 ± 47.5	204.2 ± 52.1	Anaerobic
*Lm*FH-2	Fumarate	1.9 ± 0.3	44.3 ± 4.9	48.6 ± 5.4	Aerobic
*Lm*FH-1	S-Malate	2.3 ± 0.3	11.8 ± 1.2	12.9 ± 1.3	Anaerobic
*Lm*FH-1	S-Malate	1.2 ± 0.3	0.50 ± 0.03	0.55 ± 0.03	Aerobic
*Lm*FH-2	S-Malate	12.6 ± 2.7	138.1 ± 18.7	151.4 ± 20.5	Anaerobic
*Lm*FH-2	S-Malate	5.7 ± 0.2	22.7 ± 0.5	24.9 ± 0.5	Aerobic

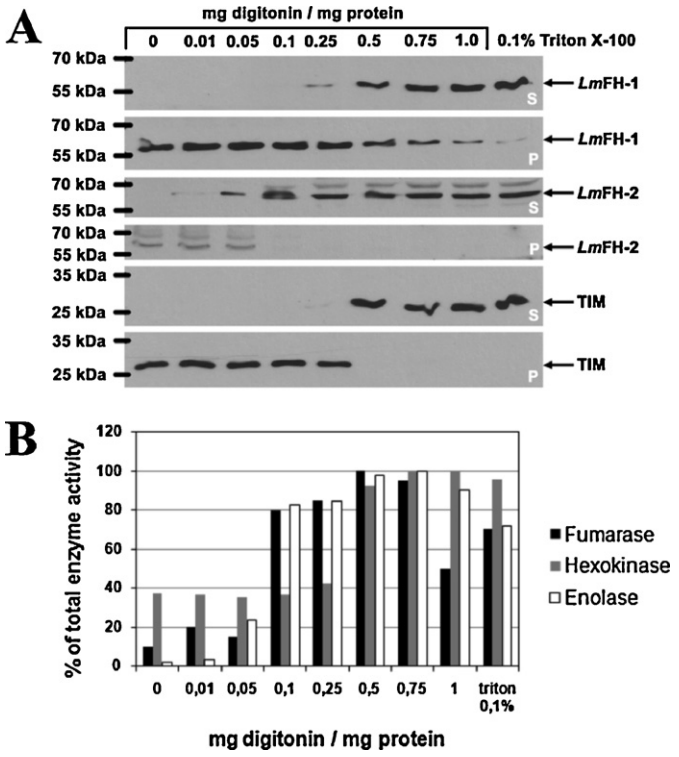

Fig. 2. Subcellular localization of *Lm*FH isoforms in *L. mexicana* promastigotes by digitonin titration. (A) Western blot probed with the polyclonal antibodies anti-*Lm*FH-1, anti-*Lm*FH-2 and anti-TIM to detect, respectively, *Lm*FH-1 (61.1 kDa), *Lm*FH-2 (62.6 kDa) and TIM (27 kDa) in supernatants (S) and pellets (P) obtained after treatment of the parasites with digitonin at the indicated concentrations. (B) Enzymatic activity of fumarate hydratase, hexokinase and enolase from soluble cell fractions obtained after treatment of the cells with digitonin.

fumarate hydratase also in the glycosomes. About 40% of the hexokinase activity was found in the supernatant fraction, even without detergent addition. This activity should possibly be attributed to the hexokinase that has been reported to be associated with the outer surface of *Leishmania* promastigotes, in the flagellar pocket, and claimed to act as a hemoglobin acceptor [36].

Western blot analyses of the soluble fractions by using antisera to the *Lm*FH isoforms indicated that essentially all *Lm*FH-2 was released already at low digitonin concentrations, confirming its cytosolic localization. However, an additional glycosomal localization of a small amount of this isoform, as found by activity assays, could not be confirmed by immunoblotting. Western blot analyses of the soluble fractions indicated that *Lm*FH-1 was only released when detergent levels reached 0.25 mg of digitonin per mg of protein and that *Lm*FH-1 is still present in insoluble fractions even at higher concentrations. These analyses suggested the mitochondrial compartmentalization of *Lm*FH-1 isoform, which is in agreement with *in silico* analysis that indicates the presence of a mitochondrial transit peptide [25].

The multiple subcellular localization of both *Lm*FH isoforms was also confirmed by immunofluorescence microscopy using specific anti-*Lm*FH-1 and anti-*Lm*FH-2 sera (Fig. 3). This microscopy analysis of the *L. mexicana* promastigotes showed that *Lm*FH-1 was clearly detected with a typical mitochondrial localization. This localization was evidenced by the intense yellow merge signal, which corresponds to the co-localization of *Lm*FH-1 (green fluorescence pattern) with the red mitochondrial marker (Mito-tracker) (Fig. 3A). Immunofluorescence studies of *Lm*FH-2 showed a diffuse pattern characteristic of a cytosolic localization, and suggested also a punctate pattern that may be characteristic of a glycosomal localization. In addition, *Lm*FH-2 did not co-localize with the mitochondria (Fig. 3B). Thus, our results indicate that *Lm*FH-1 is found in the mitochondrion whereas *Lm*FH-2 is located in the cytosol and possibly some of it also in glycosomes. This possibly dual localization of *Lm*FH-2 may be correlated to the presence of a cryptic PST1 glycosomal-targeting motif at the C-terminal extremity (SKTLA) that may, under certain conditions, be decrypted to become a functional PTS as suggested previously [26].

*Lm*FH isoforms are important for the energy metabolism in *Leishmania* through the production of fumarate in cytosol, glycosomes and mitochondrion. Fumarate has an important role in several steps of the intermediary metabolism of trypanosomatids. In the cytosol, fumarate acts as a substrate of dihydroorotate dehydrogenase, an enzyme that participates in the *de novo* pyrimidine biosynthesis pathway [14]. In mitochondrion and glycosomes, fumarate may, like in procyclic *T. brucei*, participate in the succinic fermentation pathways acting as a substrate of the mitochondrial [37] and glycosomal [16] isoforms of fumarate reductase, respectively. Contrary to the situation in *T. brucei* where no TCA cycle activity has been detected and instead parts of the cycle act independently [38], *Lm*FH-1 may also participate in the TCA cycle to

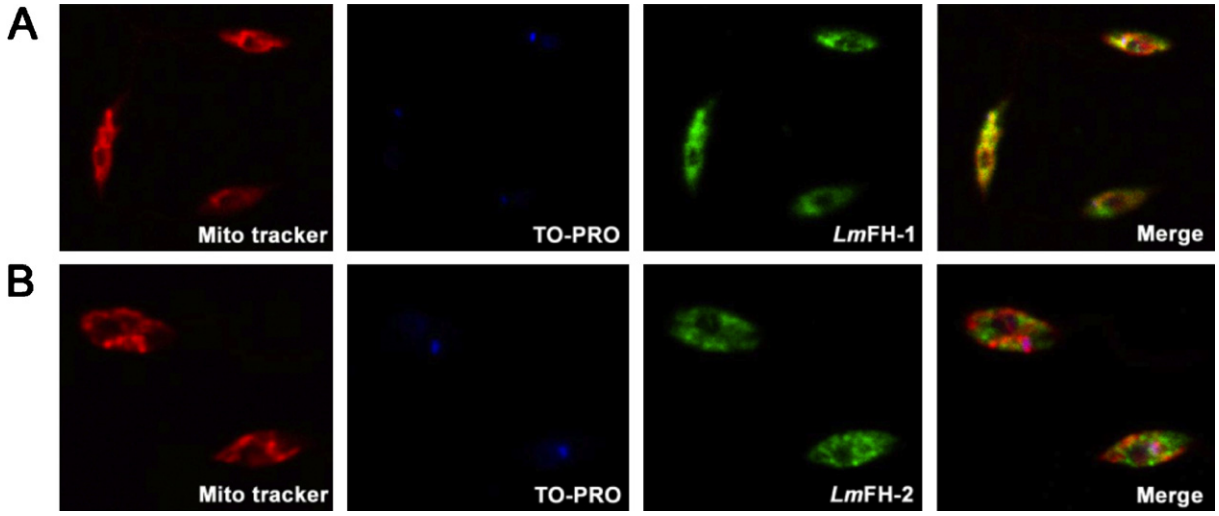

Fig. 3. Subcellular localization of *Lm*FH isoforms in *L. mexicana* promastigotes by immunofluorescence microscopy. Mitochondria are labeled in red with Mito-tracker, DNA in blue with TO-PRO, *Lm*FH-1 (A) and *Lm*FH-2 (B) in green with anti-*Lm*FH-1 and anti-*Lm*FH-2 respectively, by using Alexa Fluor 488 anti-rabbit as the secondary antibody. (For interpretation of the references to color in this figure legend, the reader is referred to the web version of the article.)

catalyze the reversible reaction of fumarate to malate. Recent studies showed that the full catabolism of glucose to carbon dioxide, through the operation of a complete TCA cycle, is essential for the growth of *Leishmania* promastigotes [39].

The vital role of fumarate hydratases in a wide range of cellular processes: pyrimidine biosynthesis, succinic fermentation and TCA cycle, as well as the fact that fumarate hydratases from different *Leishmania* species share very high sequence identity indicate that fumarate hydratases may be considered for exploitation as targets for the development of antileishmanial drugs. The development of a protocol to overproduce soluble and active enzymes, in conjunction with the results from the structural, kinetics and subcellular localization experiments presented in this paper, provides an important basis for further crystallographic and functional studies. Work on these topics is currently in progress.

Acknowledgments

We thank Melisa Gualdrón-López for help in some experiments. The authors are grateful to Prof. Otávio Thiemann (Universidade de São Paulo, São Carlos-SP, Brazil) for providing *L. major* DNA. This work received financial support from Fundação de Amparo a Pesquisa do Estado de São Paulo (FAPESP), Grants 2006/05538-5 and 2009/10454-3 (PRF), 2009/15810-2 (FD) and 2008/08262-6 (MCN). SG acknowledges a 'Maurange' postdoctoral fellowship from the 'de Duve Institute'.

Appendix A. Supplementary data

Supplementary data associated with this article can be found, in the online version, at http://dx.doi.org/10.1016/j.ijbiomac.2012.04.025.

References

[1] B.L. Herwaldt, Lancet 354 (1999) 1191–1199.
[2] H.W. Murray, J.D. Berman, C.R. Davies, N.G. Saravia, Lancet 366 (2005) 1561–1577.
[3] L. Kedzierski, A. Sakthianandeswaren, J.M. Curtis, P.C. Andrews, P.C. Junk, K. Kedzierska, Current Medicinal Chemistry 16 (2009) 599–614.
[4] A.C. Ivens, C.S. Peacock, E.A. Worthey, L. Murphy, G. Aggarwal, M. Berriman, E. Sisk, M.A. Rajandream, E. Adlem, R. Aert, A. Anupama, Z. Apostolou, P. Attipoe, N. Bason, C. Bauser, A. Beck, S.M. Beverley, G. Bianchettin, K. Borzym, G. Bothe, C.V. Bruschi, M. Collins, E. Cadag, L. Ciarloni, C. Clayton, R.M.R. Coulson, A. Cronin, A.K. Cruz, R.M. Davies, J. De Gaudenzi, D.E. Dobson, A. Duesterhoeft, G. Fazelina, N. Fosker, A.C. Frasch, A. Fraser, M. Fuchs, C. Gabel, A. Goble, A. Goffeau, D. Harris, C. Hertz-Fowler, H. Hilbert, D. Horn, Y.T. Huang, S. Klages, A. Knights, M. Kube, N. Larke, L. Litvin, A. Lord, T. Louie, M. Marra, D. Masuy, K. Matthews, S. Michaeli, J.C. Mottram, S. Muller-Auer, H. Munden, S. Nelson, H. Norbertczak, K. Oliver, S. O'Neil, M. Pentony, T.M. Pohl, C. Price, B. Purnelle, M.A. Quail, E. Rabbinowitsch, R. Reinhardt, M. Rieger, J. Rinta, J. Robben, L. Robertson, J.C. Ruiz, S. Rutter, D. Saunders, M. Schafer, J. Schein, D.C. Schwartz, K. Seeger, A. Seyler, S. Sharp, H. Shin, D. Sivam, R. Squares, S. Squares, V. Tosato, C. Vogt, G. Volckaert, R. Wambutt, T. Warren, H. Wedler, J. Woodward, S.G. Zhou, W. Zimmermann, D.F. Smith, J.M. Blackwell, K.D. Stuart, B. Barrell, P.J. Myler, Science 309 (2005) 436–442.
[5] C.S. Peacock, K. Seeger, D. Harris, L. Murphy, J.C. Ruiz, M.A. Quail, N. Peters, E. Adlem, A. Tivey, M. Aslett, A. Kerhornou, A. Ivens, A. Fraser, M.A. Rajandream, T. Carver, H. Norbertczak, T. Chillingworth, Z. Hance, K. Jagels, S. Moule, D. Ormond, S. Rutter, R. Squares, S. Whitehead, E. Rabbinowitsch, C. Arrowsmith, B. White, S. Thurston, F. Bringaud, S.L. Baldauf, A. Faulconbridge, D. Jeffares, D.P. Depledge, S.O. Oyola, J.D. Hilley, L.O. Brito, L.R.O. Tosi, B. Barrell, A.K. Cruz, J.C. Mottram, D.F. Smith, M. Berriman, Nature Genetics 39 (2007) 839–847.
[6] R.L. Coppel, C.G. Black, International Journal for Parasitology 35 (2005) 465–479.
[7] S.A. Woods, S.D. Schwartzbach, J.R. Guest, Biochimica et Biophysica Acta 954 (1988) 14–26.
[8] H. Shibata, W.E. Gardiner, S.D. Schwartzbach, Journal of Bacteriology 164 (1985) 762–768.
[9] T. Suzuki, M. Sato, T. Yoshida, S. Tuboi, Journal of Biological Chemistry 264 (1989) 2581–2586.
[10] B.T. Kinsella, S. Doonan, Bioscience Reports 6 (1986) 921–929.
[11] B.M.A. van Vugt-Lussenburg, L. van der Weel, W.R. Hagen, P.L. Hagedoorn, Microbiology-SGM 155 (2009) 3015–3020.
[12] T. Shimoyama, E. Rajashekhara, D. Ohmori, T. Kosaka, K. Watanabe, FEMS Microbiology Letters 270 (2007) 207–213.
[13] E. Takashima, D.K. Inaoka, A. Osanai, T. Nara, M. Odaka, T. Aoki, K. Inaka, S. Harada, K. Kita, Molecular and Biochemical Parasitology 122 (2002) 189–200.
[14] P.R. Feliciano, A.T. Cordeiro, A.J. Costa, M.C. Nonato, Protein Expression and Purification 48 (2006) 98–103.
[15] O. Yogev, E. Singer, E. Shaulian, M. Goldberg, T.D. Fox, O. Pines, PLoS Biology 8 (2010).
[16] S. Besteiro, M. Biran, N. Biteau, V. Coustou, T. Baltz, P. Canioni, F. Bringaud, Journal of Biological Chemistry 277 (2002) 38001–38012.
[17] T. Bourgeron, D. Chretien, J. Poggibach, S. Doonan, D. Rabier, P. Letouze, A. Munnich, A. Rotig, P. Landrieu, P. Rustin, Journal of Clinical Investigation 93 (1994) 2514–2518.
[18] V. Coustou, M. Biran, S. Besteiro, L. Riviere, T. Baltz, J.M. Franconi, F. Bringaud, Journal of Biological Chemistry 281 (2006) 26832–26846.
[19] D. Hanahan, Journal of Molecular Biology 166 (1983) 557–580.
[20] S. Jaganaman, A. Pinto, M. Tarasev, D.P. Ballou, Protein Expression and Purification 52 (2007) 273–279.
[21] C.N. Pace, F.X. Schmidt, in: T.E. Creighton (Ed.), Protein Structure: A Practical Approach, second ed., IRL Press, New York, 1997, pp. 253–259.
[22] M.M. Bradford, Analytical Biochemistry 72 (1976) 248–254.
[23] O. Misset, F.R. Opperdoes, European Journal of Biochemistry 144 (1984) 475–483.
[24] V. Hannaert, M.A. Albert, D.J. Rigden, M.T.D. Giotto, O. Thiemann, R.C. Garratt, J. Van Roy, F.R. Opperdoes, P.A.M. Michels, European Journal of Biochemistry 270 (2003) 3205–3213.
[25] F.R. Opperdoes, J.P. Szikora, Molecular and Biochemical Parasitology 147 (2006) 193–206.
[26] P.A.M. Michels, F. Bringaud, M. Herman, V. Hannaert, Biochimica et Biophysica Acta: Molecular Cell Research 1763 (2006) 1463–1477.
[27] C. Perez-Iratxeta, M.A. Andrade-Navarro, BMC Structural Biology 8 (2008).
[28] M. Barteri, M. Diociaiuti, A. Pala, S. Rotella, Biophysical Chemistry 111 (2004) 35–42.
[29] T. Mizobata, T. Fujioka, F. Yamasaki, M. Hidaka, J. Nagai, Y. Kawata, Archives of Biochemistry and Biophysics 355 (1998) 49–55.
[30] S. Colombo, M. Grisa, P. Tortora, M. Vanoni, FEBS Letters 337 (1994) 93–98.
[31] W. Lin, M. Chan, L.-L. Goh, T.-S. Sim, Applied Microbiology and Biotechnology 75 (2007) 329–335.
[32] B.L.M. VanKuijk, N.D. VanLoo, A.F. Arendsen, W.R. Hagen, A.J.M. Stams, Archives of Microbiology 165 (1996) 126–131.
[33] D.H. Flint, Archives of Biochemistry and Biophysics 311 (1994) 509–516.
[34] A. Leroux, X. Fleming-Canepa, A. Aranda, D. Maugeri, J.J. Cazzulo, M.A. Sanchez, C. Nowicki, Molecular and Biochemical Parasitology 149 (2006) 74–85.
[35] D.H. Flint, M.H. Emptage, J.R. Guest, Biochemistry 31 (1992) 10331–10337.
[36] G. Krishnamurthy, R. Vikram, S.B. Singh, N. Patel, S. Agarwal, G. Mukhopadhyay, S.K. Basu, A. Mukhopadhyay, Journal of Biological Chemistry 280 (2005) 5884–5891.
[37] V. Coustou, S. Besteiro, L. Riviere, M. Biran, N. Biteau, J.M. Franconi, M. Boshart, T. Baltz, F. Bringaud, Journal of Biological Chemistry 280 (2005) 16559–16570.
[38] S.W.H. van Weelden, J.J. van Hellemond, F.R. Opperdoes, A.G.M. Tielens, Journal of Biological Chemistry 280 (2005) 12451–12460.
[39] E.C. Saunders, W.W. Ng, J.M. Chambers, M. Ng, T. Naderer, J.O. Kroemer, V.A. Likic, M.J. McConville, Journal of Biological Chemistry 286 (2011) 27706–27717.